

The Inability of Ambipolar Diffusion to set a Characteristic Mass Scale in Molecular Clouds

Jeffrey S. Oishi^{1,2}

joishi@amnh.org

Mordecai-Mark Mac Low²

mordecai@amnh.org

ABSTRACT

We investigate the question of whether ambipolar diffusion (ion-neutral drift) determines the smallest length and mass scale on which structure forms in a turbulent molecular cloud. We simulate magnetized turbulence in a mostly neutral, uniformly driven, turbulent medium, using a three-dimensional, two-fluid, magnetohydrodynamics (MHD) code modified from Zeus-MP. We find that substantial structure persists below the ambipolar diffusion scale because of the propagation of compressive slow MHD waves at smaller scales. Contrary to simple scaling arguments, ambipolar diffusion thus does not suppress structure below its characteristic dissipation scale as would be expected for a classical diffusive process. We have found this to be true for the magnetic energy, velocity, and density. Correspondingly, ambipolar diffusion leaves the clump mass spectrum unchanged. Ambipolar diffusion appears unable to set a characteristic scale for gravitational collapse and star formation in turbulent molecular clouds.

Subject headings: ISM: clouds – ISM: kinematics and dynamics – ISM: magnetic fields – MHD – stars: formation – turbulence

1. Introduction

Molecular clouds are turbulent, with linewidths indicating highly supersonic motions (Zuckerman & Palmer 1974), and magnetized, with magnetic energies in or near equipartition

¹Department of Astronomy, University of Virginia, P.O. Box 3818, Charlottesville, VA 22903

²Department of Astrophysics, American Museum of Natural History, New York, NY 10024-5192

with thermal energy (Crutcher 1999). They have low ionization fractions (Elmegreen 1979) leading to imperfect coupling of the magnetic field with the gas. Molecular clouds are the sites of all known star formation, so characterizing the properties of this non-ideal, magnetized turbulence appears central to formulating a theory of star formation.

The drift of an ionized, magnetized gas through a neutral gas coupled to it by ion-neutral collisions is known by astronomers as ambipolar diffusion (AD) and by plasma physicists as ion-neutral drift. It was first proposed in an astrophysical context by Mestel & Spitzer (1956) as a mechanism for removing magnetic flux and hence magnetic pressure from collapsing protostellar cores in the then-novel magnetic field of the Galaxy. However, more recently, as turbulence has regained importance in the theory of star formation, AD has been invoked as a source of dissipation for magnetic energy in the turbulent magnetohydrodynamic (MHD) cascade and thus a characteristic length scale for the star formation process (e.g., Tassis & Mouschovias 2004). This is due to its well-known ability to damp certain families of linear MHD waves (Kulsrud & Pearce 1969; Ferrière, Zweibel, & Shull 1988; Balsara 1996). However, as Balsara (1996) pointed out, AD does allow slow modes to propagate undamped.

A brief calculation suggests that AD should be the most important dissipation mechanism in molecular clouds. AD can be expressed as an additional force term in the momentum equation for the ions

$$F_{in} = \rho_i \rho_n \gamma_{AD} (\mathbf{v}_n - \mathbf{v}_i), \quad (1)$$

and an equal and opposite force $F_{ni} = -F_{in}$ in the neutral momentum equation, where ρ_i and ρ_n are the ion and neutral densities and $\gamma_{AD} \simeq 9.2 \times 10^{13} \text{ cm}^3 \text{ s}^{-1} \text{ g}^{-1}$ is the collisional coupling constant (Draine, Roberge, & Dalgarno 1983; Smith & Mac Low 1997).

The effect of ion-neutral drift on the magnetic field can be simply expressed in the strong coupling approximation (Shu 1983) that neglects the momentum and pressure of the ion fluid and equates the collisional drag force on the ions F_{in} with the Lorentz force,

$$-\rho_i \rho_n \gamma_{AD} (\mathbf{v}_i - \mathbf{v}_n) = \frac{(\nabla \times \mathbf{B}) \times \mathbf{B}}{4\pi}. \quad (2)$$

Brandenburg & Zweibel (1994) note that by substituting equation (2) into the induction equation for the ions, one arrives at

$$\partial_t \mathbf{B} = \nabla \times \left[(\mathbf{v}_n \times \mathbf{B}) + \frac{(\nabla \times \mathbf{B}) \cdot \mathbf{B}}{4\pi \rho_i \rho_n \gamma_{AD}} \mathbf{B} - (\eta + \eta_{AD}) \nabla \times \mathbf{B} \right], \quad (3)$$

where

$$\eta_{AD} = \frac{B^2}{4\pi \rho_i \rho_n \gamma_{AD}} \quad (4)$$

is the ambipolar diffusivity and η is the Ohmic diffusivity. However, dissipation is not the only contribution of AD to the induction equation. Given that AD tends to force magnetic

fields into force-free states (Brandenburg et al. 1995; Zweibel & Brandenburg 1997) with $(\nabla \times \mathbf{B}) \times \mathbf{B} = 0$, it should come as little surprise that the $(\nabla \times \mathbf{B}) \cdot \mathbf{B}$ term must be given proper consideration.

We can approximate the scale ℓ_{ds} below which dissipation dominates turbulent structure for a given diffusivity η in at least two ways. The first is commonly used in the turbulence community. It is to equate the driving timescale

$$\tau_{dr} = L_{dr}/v_{dr}, \quad (5)$$

where L_{dr} is the driving wavelength and v_{dr} is the rms velocity at that wavelength, with the dissipation timescale $\tau_{ds} = \ell_{ds}^2/\eta$, and solve for ℓ_{ds} . The second method was suggested by Balsara (1996) and Zweibel & Brandenburg (1997) and advocated by Klessen et al. (2000). It is to estimate the length scale at which the Reynolds number associated with a given dissipation mechanism becomes unity. The Reynolds number for ion-neutral drift can be defined as

$$R_{AD} = \frac{LV}{\eta_{AD}}, \quad (6)$$

where V is a characteristic velocity. This method requires setting R_{AD} to one and solving for $L = \ell_{ds}$ to find

$$\ell_{AD} = \frac{B^2}{4\pi\rho_i\rho_n\gamma_{AD}V}. \quad (7)$$

Klessen et al. (2000) show that by adopting values characteristic of dense molecular clouds, a magnetic field strength $B = 10B_{10} \mu\text{G}$, ionization fraction $x = 10^{-6}x_6$, neutral number density $n_n = 10^3n_3 \text{ cm}^{-3}$, mean mass per particle $\mu = 2.36m_H$ where m_H is the hydrogen mass, such that $\rho_n = \mu n_n$, and the above value for the ion-neutral coupling constant, the length scale at which AD is important is given by

$$\ell_{AD} = (0.04 \text{ pc}) \frac{B_{10}}{M_A x_6 n_3^{3/2}}, \quad (8)$$

where $M_A = V/v_A$ is the Alfvén Mach number. By contrast, Ohmic dissipation acts only at far smaller scales, $\ell_\eta \sim 10^{-13} \text{ pc}$ (Zweibel & Brandenburg 1997).

For our purposes, we use the Reynolds number method and choose $V = v_{RMS}$, the RMS velocity. Although we use Reynolds numbers, we find that using the timescale method has no effect on our results.

Previous three-dimensional numerical studies of turbulent ion-neutral drift have used the strong coupling approximation (Padoan, Zweibel, & Nordlund 2000). This by definition renders simulations unable to reach below $R_{AD} \sim 1$, and thus into the dissipation region.

In this paper, we present runs in which we vary the ambipolar diffusion coupling constant, and thus ℓ_{AD} . We find a surprising lack of dependence of the spectral properties on the strength of the ambipolar diffusivity. In particular, no new dissipation range is introduced into the density, velocity or magnetic field spectra by ambipolar diffusion, nor is the clump mass spectrum materially changed.

2. Numerical Method

We solve the two-fluid equations of MHD using the ZEUS-MP code (Norman 2000) modified to include a semi-implicit treatment of ion-neutral drift. ZEUS-MP is the domain-decomposed, parallel version of the well-known shared memory code ZEUS-3D (Clarke & Norman 1994). Both codes follow the algorithms of ZEUS-2D (Stone & Norman 1992a,b), including van Leer (1977) advection, and the constrained transport method of characteristics (Evans & Hawley 1988; Hawley & Stone 1995) for the magnetic fields. We add an additional neutral fluid and collisional coupling terms to both momentum equations. Because ion-neutral collisions constitute a stiff term, we evaluate the momentum equations using the semi-implicit algorithm of Mac Low & Smith (1997). We also include an explicit treatment of Ohmic diffusion by operator splitting the induction equation (Fleming, Stone, & Hawley 2000).

We ignore ionization and recombination, assuming that such processes take place on timescales much longer than the ones we are concerned with. This means that ions and neutrals are separately conserved. Furthermore, we assume that both fluids are isothermal and at the same temperature, thus sharing a common sound speed c_s .

2.1. Initial Conditions and Parameters

All of our runs are on three-dimensional Cartesian grids with periodic boundary conditions in all directions.

The turbulence is driven by the method detailed in Mac Low (1999). Briefly, we generate a top hat function in Fourier space between $1 < |k| < 2$. The amplitudes and phases of each mode are chosen at random, and once returned to physical space, the resulting velocities are normalized to produce the desired RMS velocity, unity in our case. At each timestep, the same pattern of velocity perturbations is renormalized to drive the box with a constant energy input ($\dot{E} = 1.0$ for all simulations) and applied to the neutral gas.

Our isothermal sound speed is $c_s = 0.1$, corresponding to an initial RMS Mach number

$M = 10$. The initial neutral density ρ_n is everywhere constant and set to unity. The magnetic field strength is set by requiring that the initial ratio of gas pressure to magnetic pressure be everywhere $\beta = 8\pi c_s^2 \rho / B^2 = 0.1$; its direction lies along the z-axis.

Although our semi-implicit method means that the timestep is not restricted by the standard Courant condition for diffusive processes (that is, $\propto [\Delta x]^2$), the two-fluid model is limited by the Alfvén timestep for the ions. This places strong constraints on the ionization fraction ($x = n_i/n_n$) we can reasonably compute. We therefore adapt a fixed fraction of $x = 0.1$ for our simulations. While this fraction is certainly considerably higher than the 10^{-4} – 10^{-9} typical of molecular clouds, the ionization fraction only enters the calculation in concert with the collisional coupling constant γ_{AD} . Thus, we are able to compensate for the unrealistically high ionization fraction by adjusting γ_{AD} accordingly.

We present four runs, two with AD, one with Ohmic diffusion, and one ideal MHD run (see Table 1). For the AD runs, we vary the collisional coupling constant in order to change the diffusivity.

Our results are reported for a resolution of 256^3 at time $t = 0.125t_s = 2.5$ where $t_s = 20$ is the sound crossing time for the box. This exceeds by at least 30% the turbulent crossing time over the driving scale τ_{dr} computed from equation (5), and tabulated in Table 1. Our computation of τ_{dr} is done for $L_{dr} = 1$, the maximum driving wavelength. Vestuto, Ostriker, & Stone (2003) note that τ_{dr} is the relevant timescale for the formation of nonlinear structures. Furthermore, we find from studies performed at 128^3 out to $t = 0.3t_s$ that $0.125t_s$ is enough time to reach a steady state in energy.

3. Results

Figure 1 shows cuts of density perpendicular and parallel to the mean magnetic field. For the ambipolar diffusion runs, we show the total density $\rho = \rho_i + \rho_n$. The morphology of density enhancements in the different runs appears similar, giving a qualitative suggestion of the quantitative results on clump mass spectra discussed next.

3.1. Clump mass spectrum

We wish to understand whether AD determines the smallest scale at which clumps can form in turbulent molecular clouds. Determining structure within molecular clouds has proved difficult in both theory and observation. Molecular line maps (eg, Falgarone et al 1992) show that for all resolvable scales, the density fields of clouds is made up of a hierarchy

of clumps. Furthermore, the identification of clumps projected on the sky with physical volumetric objects is questionable (Ostriker, Stone, & Gammie 2001; Ballesteros-Paredes & Mac Low 2002).

Nonetheless, density enhancements in a turbulent flow likely provide the initial conditions for star formation. To clarify the effects of different turbulent dissipation mechanisms on the clump mass spectrum, we study our three dimensional simulations of turbulence without gravity. By using the CLUMPFIND algorithm (Williams, de Geus, & Blitz 1994) on the density field to identify contiguous regions of enhanced density, we can construct a clump mass spectrum (Fig. 2). Although such methods are parameter-sensitive when attempting to draw comparisons to observed estimates for the clump-mass spectrum (Ballesteros-Paredes & Mac Low 2002), we are only interested in using the mass spectrum as a point of comparison between runs with different dissipative properties.

For this section, we dimensionalize our density field following Mac Low (1999), with a length scale $L' = 0.5$ pc, and mean density scale $\rho'_0 = 10^4(2m_H)$ g cm $^{-3}$ in order to present results in physical units relevant to star formation.

We search for clumps above a density threshold set at $5\langle\rho\rangle$ (where in the AD cases $\rho = \rho_i + \rho_n$) and bin the results by mass to produce a clump-mass spectrum. Figure 2 shows that while Ohmic diffusion has a dramatic effect on the number of low-mass clumps, AD has nearly none. Although there are small fluctuations around the hydrodynamic spectrum, there is no systematic trend with increasing strength of AD. This result suggests that AD does not control the minimum mass of clumps formed in turbulent molecular clouds.

3.2. Magnetic Energy and Density Spectra

The lack of an effect on the clump mass spectrum can be better understood by examining the distribution of magnetic field and density.

AD produces no evident dissipation range in the magnetic energy spectrum. As seen in Figure 3, for two different values of ambipolar diffusivity η_{AD} , the power spectrum of magnetic field retains the shape of the ideal run. For comparison, we have also plotted the run with Ohmic diffusion. While the expected dissipation wavenumbers (determined in both cases by the Reynolds number method mentioned above) of the $\eta_{AD} = 0.275$ and $\eta = 0.250$ runs are very similar, the effect of Ohmic diffusion is quite apparent in the declining slope of the magnetic energy spectrum, in contrast to AD.

The total power does decrease as the ambipolar diffusivity η_{AD} increases. Because we

drive only the neutrals, this could be interpreted as magnetic energy being lost during the transfer of driving energy from the ions to the neutrals via the coupling. However, we performed a simulation in which both ions and neutrals were driven with the same driving pattern and found almost no difference in the power spectra from our standard (neutral driving only) case.

We instead suspect that the decline in total magnetic energy occurs because AD does damp some families of MHD waves, notably Alfvén waves (Kulsrud & Pearce 1969), even though it does not introduce a characteristic damping scale.

In order to demonstrate this, the flow will need to be decomposed into its constituent MHD wave motions at each point in space. Such a technique has been used before by Maron & Goldreich (2001) for incompressible MHD turbulence and by Cho & Lazarian (2002) for compressible MHD turbulence. The technique used by Cho & Lazarian (2002) decomposes wave motions along a mean field assumed to be present. However, because the local field is distorted by the turbulence and thus not necessarily parallel to the mean, a mean-field decomposition tends to spuriously mix Alfvén and slow modes (Maron & Goldreich 2001). If the local field line distortion is great enough, the decomposition must be made with respect to the local field, a much more demanding procedure. Although wave decomposition analysis is outside the scope of this paper, it remains a fruitful avenue for future research.

In order to ensure that the lack of spectral features seen in the magnetic spectrum (and similarly in the density spectrum) is not an artifact of the limited inertial range in our simulations, we ran our $\eta_{AD} = 0.275$ (medium collision strength) case at resolutions of 64^3 , 128^3 , and 256^3 . Figure 4 demonstrates that increasing the resolution increases the inertial range, but does not resolve any noticeable transition to dissipation at the AD length, suggesting that our results are not sensitive to the resolution.

Figure 5 shows the spectrum of the density for all runs. In the case of the AD runs, we use the sum of the neutral and ion density.

The density spectrum peaks at small scale in compressible turbulence (Joung & Mac Low 2005). Varying the ambipolar diffusivity by a factor of two makes little systematic difference to the shape of the density spectrum. It seems clear that although there are only slight differences in the density spectrum due to varying magnetic diffusivities, the density spectrum is not a particularly good indicator of underlying clump masses.

Note that we use for the density spectrum the Fourier transform of the density field rather than its square, which in the case of the magnetic field yields the one-point correlation function (or power spectrum) of the magnetic energy.

4. Discussion

Supersonic turbulence performs a dual role in its simultaneous ability to globally support a molecular cloud against gravity while at the same time producing smaller density enhancements that can sometimes gravitationally collapse (Klessen et al. 2000). While our simulations do not include gravity, it is clear that AD does not set a characteristic scale to the density field below which MHD turbulence is unable to further influence structure formation.

One of the main motivations of this study was to verify the claim made by, for example, Klessen et al. (2000) that AD sets the minimum mass for clumps in molecular cloud turbulence. However, it appears that AD is unable to set this scale, because of its selective action on different MHD waves. We do note that AD can occasionally help form magneto-hydrostatic objects in MHD turbulence, but this is not a dominant pathway, as shown by Vázquez-Semadeni et al. (2005). Although Ohmic diffusion has little trouble inhibiting low mass clump formation, it never reaches significant values at the densities where molecular clumps form.

This opens up other possibilities for the physical mechanisms determining the smallest scale fluctuations occurring in molecular clouds. An attractive option is the sonic-scale argument of Vázquez-Semadeni, Ballesteros-Paredes, & Klessen (2003), in which the length scale at which turbulent motions become incompressible, with Mach numbers dropping well below unity, determines where turbulence ceases to have an effect on the pre-stellar core distribution, and thus determines the minimum mass scale.

5. Acknowledgments

We thank J. Ballesteros-Paredes and K. Walther for collaborating on early phases of this work, and J. Maron, A. Schekochihin, J. Stone, and E. Zweibel for productive discussions. We acknowledge support from NASA grants NAG5-10103 and NAG5-13028. Computations were performed at the Pittsburgh Supercomputer Center, supported by NSF, on an Ultrasparc III cluster generously donated by Sun Microsystems, and on the Parallel Computing Facility at the American Museum of Natural History.

REFERENCES

Ballesteros-Paredes, J., & Mac Low, M.-M. 2002, *ApJ*, 570, 734

- Balsara, D. S. 1996, *ApJ*, 465, 775
- Brandenburg, A., Nordlund, Å., Stein, R. F., & Torkelsson, U. 1995, *ApJ*, 446, 741
- Brandenburg, A. & Zweibel, E. G. 1994, *ApJ*, 427, L91
- Brandenburg, A. & Zweibel, E. G. 1995, *ApJ*, 448, 734
- Cho, J., & Lazarian, A. 2002, *Physical Review Letters*, 88, 245001
- Clarke, D., & Norman, M. L. 1994, “ZEUS-3D User manual” Technical Report TR015 (National Center for Supercomputing Applications, Urbana).
- Crutcher, R. M. 1999, *ApJ*, 520, 706
- Draine, B. T., Roberge, W. G., & Dalgarno, A. 1983, *ApJ*, 264, 485
- Elmegreen, B. G., 1979, *ApJ*, 232, 729
- Evans, C. R., & Hawley, J. F. 1988, *ApJ*, 332, 659
- Ferrière, K. M., Zweibel, E. G., & Shull, J. M. 1988, *ApJ*, 332, 984
- Fleming, T. P., Stone, J. M., & Hawley, J. F. 2000, *ApJ*, 530, 464
- Hawley, J. F., & Stone, J. M. 1995, *Comp. Phys. Comm.*, 89, 127
- Joung, M. K. R., & Mac Low, M.-M. 2005, in preparation
- Klessen, R. S., Heitsch, F., & Mac Low, M.-M. 2000, *ApJ*, 535, 887
- Kulsrud, R. & Pearce, W. P. 1969, *ApJ*, 156, 445
- Mac Low, M.-M. & Klessen, R. S. 2004, *Rev. Mod. Phys.*, 76, 125
- Mac Low, M.-M. 1999, *ApJ*, 524, 169
- Mac Low, M.-M., Klessen, R. S., Burkert, A., & Smith, M. D. 1998, *Phy. Rev. Lett.*, 80, 2754
- Mac Low, M.-M. & Smith, M. D. 1997, *ApJ*, 491, 596
- Maron, J., & Goldreich, P. 2001, *ApJ*, 554, 1175
- Mestel, L. & Spitzer, L. 1956, *MNRAS*, 116, 503
- Norman, M. L. 2000, *Rev. Mex. Astron. Astrof. Conf. Ser.*, 9, 66

- Ostriker, E. C., Stone, J. M., & Gammie, C. F. 2001, *ApJ*, 546, 980
- Padoan, P., Zweibel, E. G., & Nordlund, Å. 2000, *ApJ*, 540, 332
- Shu, F. H. 1983, *ApJ*, 273, 202
- Smith, M. D., & Mac Low, M.-M. 1997, *A&A*, 326, 801
- Stone, J. M. & Norman, M. L. 1992, *ApJS*, 80, 753
- Stone, J. M. & Norman, M. L. 1992, *ApJS*, 80, 791
- Tassis, K., & Mouschovias, T. C. 2004, *ApJ*, 616, 283
- van Leer, B. 1977, *J. Comp. Phys.*, 23, 276
- Vázquez-Semadeni, E., Ballesteros-Paredes, J., & Klessen, R. S. 2003, *ApJ*, 585, L131
- Vázquez-Semadeni, E., Kim, J., Shadmehri, M., & Ballesteros-Paredes, J. 2005, *ApJ*, 618, 344
- Vestuto, J. G., Ostriker, E. C., & Stone, J. M. 2003, *ApJ*, 590, 858
- Williams, J. P., de Geus, E. J., & Blitz, L. 1994, *ApJ*, 428, 693
- Zuckerman, B., & Palmer, P. 1974, *ARA&A*, 12, 279
- Zweibel, E. G. & Brandenburg, A. 1997, *ApJ*, 478, 563

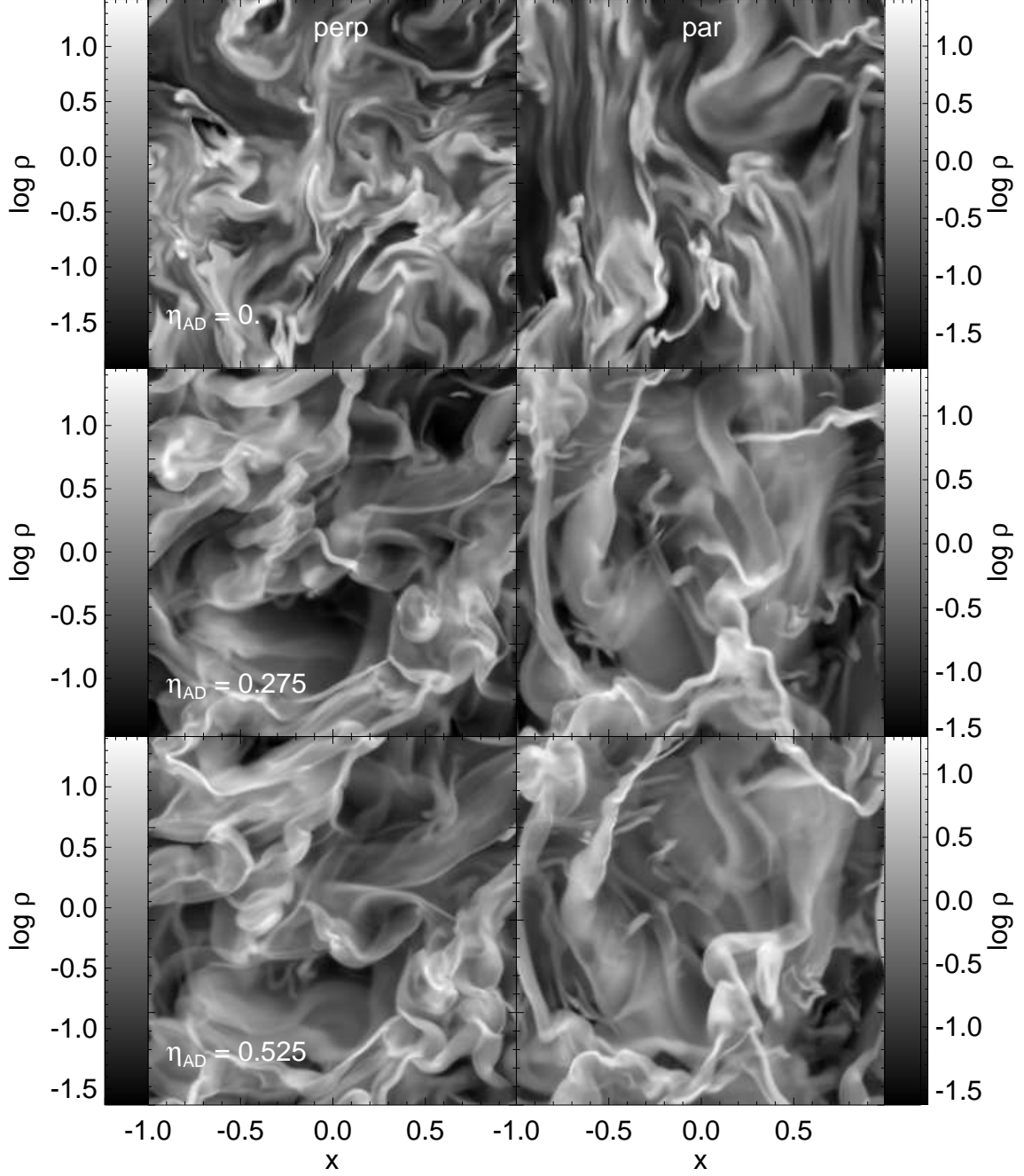


Fig. 1.— Random cuts of density ρ parallel and perpendicular to the magnetic field for each of three runs of varying ambipolar diffusivity η_{AD} . Each image is scaled to its own minimum and maximum, enhancing structural features. For AD runs, $\rho = \rho_i + \rho_n$

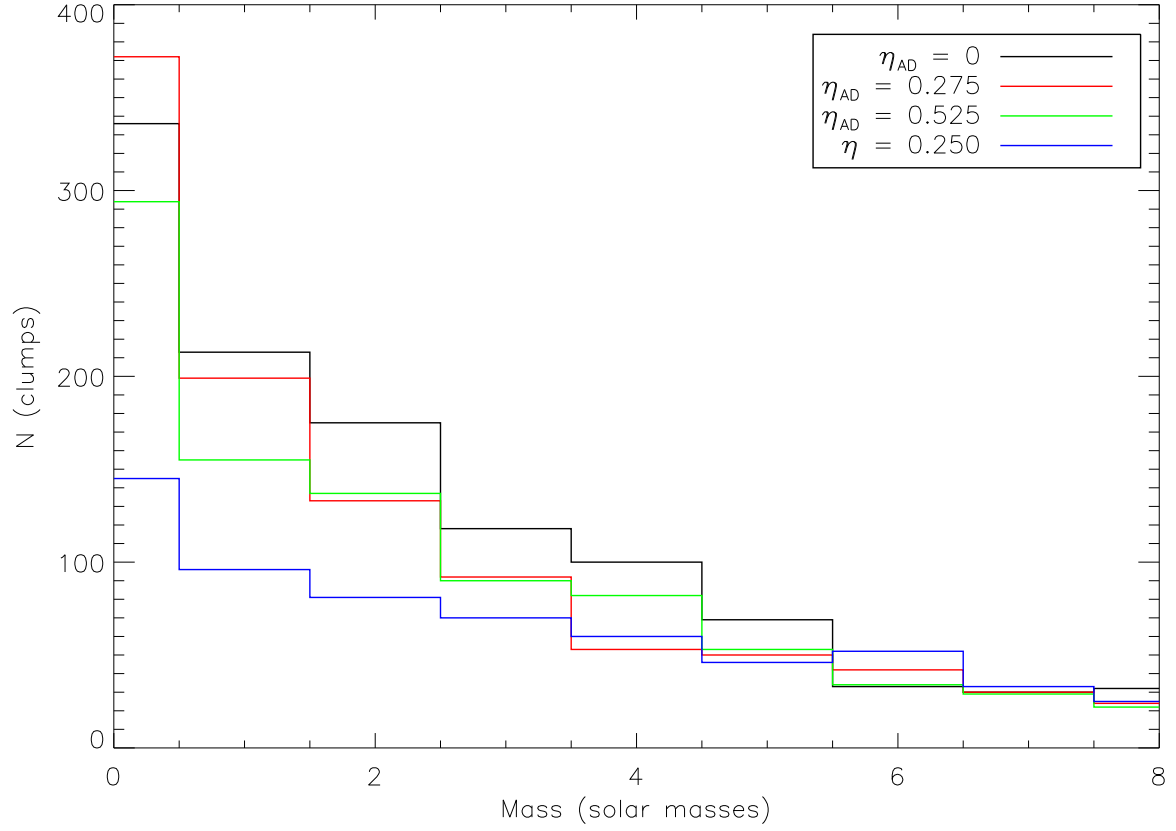


Fig. 2.— Clump mass spectrum measuring the number of clumps of a given mass for one ideal MHD run (labeled $\eta_{AD} = 0$), two AD runs ($\eta_{AD} = 0.275, 0.525$) and one Ohmic dissipation run ($\eta = 0.250$). Compare the lack of effect of AD to the significant decrease in the number of low mass clumps for the Ohmic diffusion case.

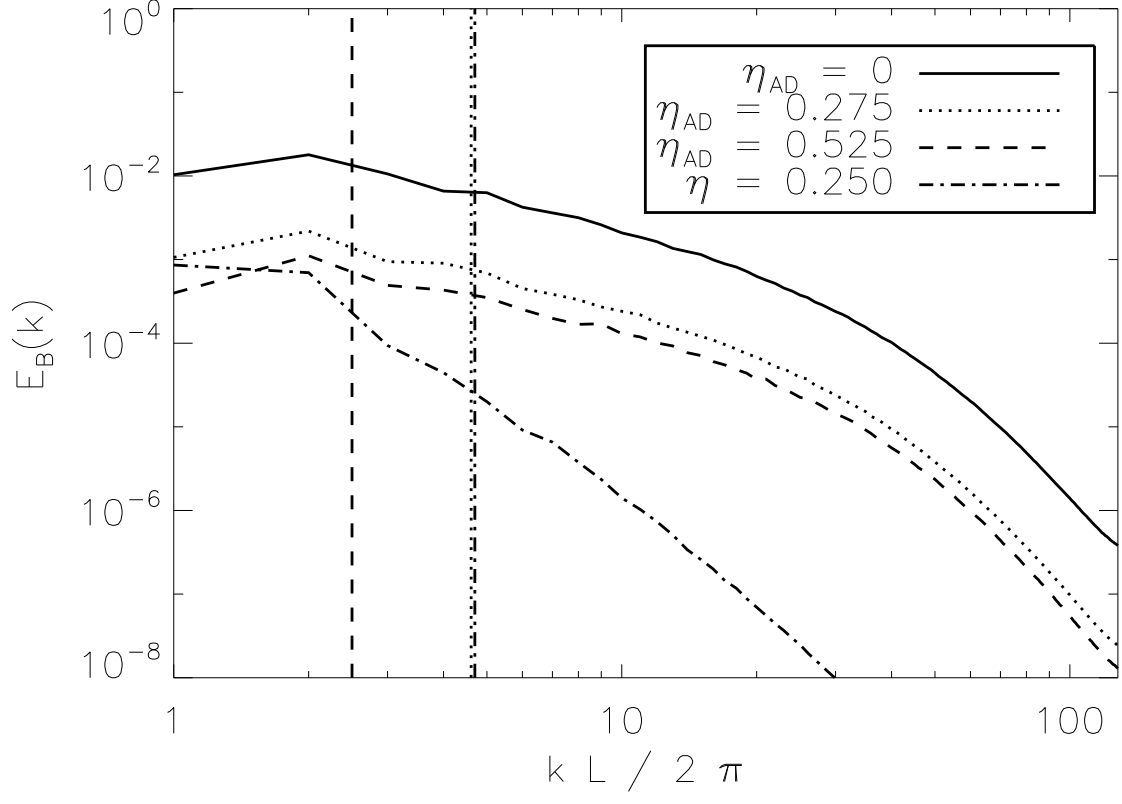


Fig. 3.— Magnetic energy spectra for the same runs as Figure 2. The vertical lines represent the wavenumber at which the AD or Ohmic Reynolds number crosses unity.

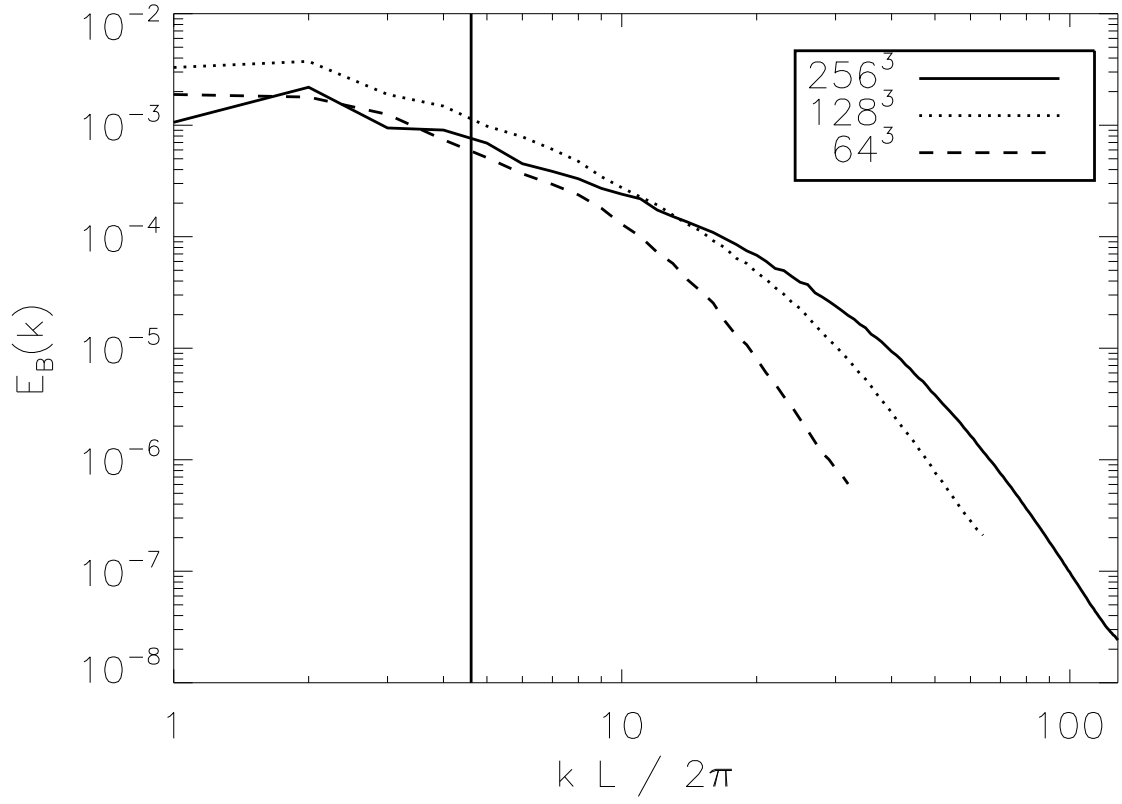


Fig. 4.— Magnetic energy spectra for three runs of varying resolution from 64^3 to 256^3 . Increased resolution shows no effects at the AD wavenumber given by the vertical line.

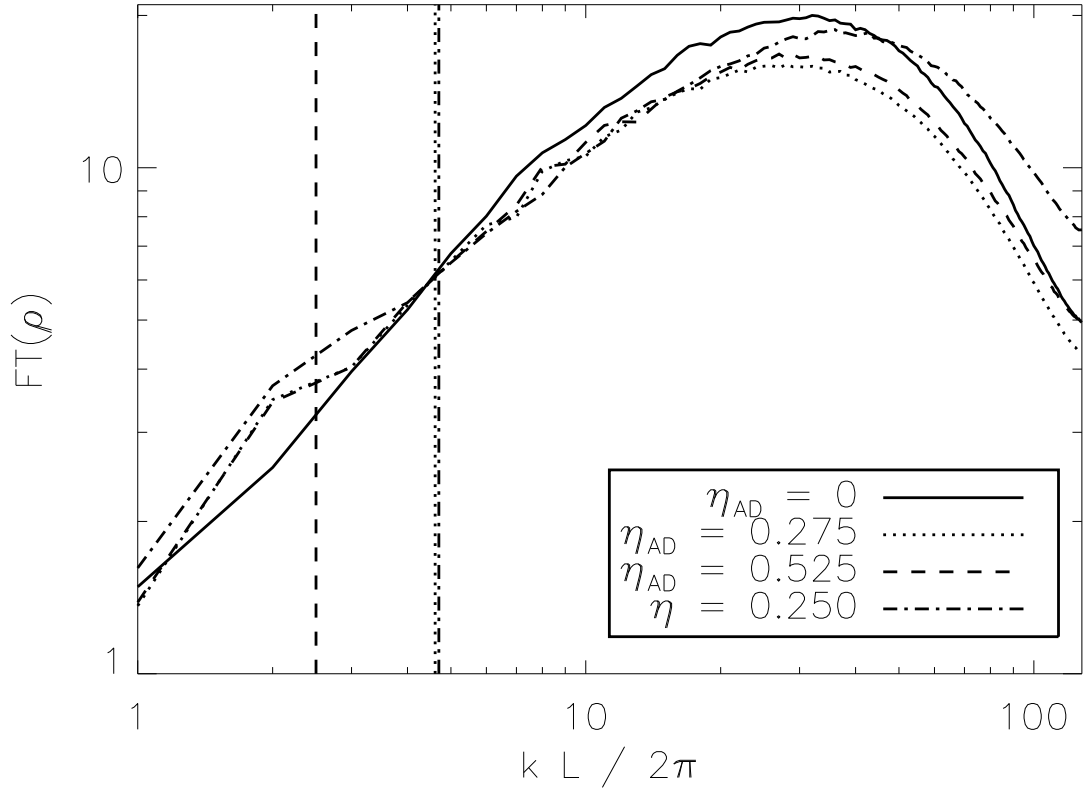


Fig. 5.— Fourier transform of density field for the same runs as Figure 2. Note that for the AD runs, this plot shows the total density, $\rho = \rho_i + \rho_n$.

Table 1. Models

Run	diffusivity	γ_{AD}	η_{AD}	η	$\sigma_{v,n}$	$\sigma_{v,i}$	τ_{dr}
A1	AD	8	0.275	0	0.603	0.526	1.66
A2	AD	4	0.575	0	0.615	0.501	1.63
O	Ohmic	0	0	0.250	-	0.577	1.73
I	-	0	0	0	-	0.630	1.59